Advances in Engineering Software 45 (2012) 203–212

Contents lists available at SciVerse ScienceDirect

Advances in Engineering Software

journal homepage: www.elsevier.com/locate/advengsoft

Genetic algorithm based support vector machine regression in predicting wave transmission of horizontally interlaced multi-layer moored floating pipe breakwater

S.G. Patil [a,*], S. Mandal [b], A.V. Hegde [c]

[a] Department of Built and Natural Environment, Caledonian College of Engineering, PO Box 2322, CPO Seeb, PC 111, Sultanate of Oman
[b] Ocean Engineering Division, National Institute of Oceanography, Goa 403 004, India
[c] Department of Applied Mechanics and Hydraulics, National Institute of Technology Karnataka, Surathkal, Srinivasnagar, Mangalore 575 025, India

ARTICLE INFO

Article history:
Received 24 May 2011
Received in revised form 23 September 2011
Accepted 24 September 2011
Available online 29 October 2011

Keywords:
Support vector machine
Genetic algorithm
Artificial neural network
ANFIS
Floating breakwater
HIMMFPB
Wave transmission

ABSTRACT

Planning and design of coastal protection works like floating pipe breakwater require information about the performance characteristics of the structure in reducing the wave energy. Several researchers have carried out analytical and numerical studies on floating breakwaters in the past but failed to give a simple mathematical model to predict the wave transmission through floating breakwaters by considering all the boundary conditions. Computational intelligence techniques, such as, Artificial Neural Networks (ANN), fuzzy logic, genetic programming and Support Vector Machine (SVM) are successfully used to solve complex problems. In the present paper, a hybrid Genetic Algorithm Tuned Support Vector Machine Regression (GA-SVMR) model is developed to predict wave transmission of horizontally interlaced multilayer moored floating pipe breakwater (HIMMFPB). Furthermore, optimal SVM and kernel parameters of GA-SVMR models are determined by genetic algorithm. The GA-SVMR model is trained on the data set obtained from experimental wave transmission of HIMMFPB using regular wave flume at Marine Structure Laboratory, National Institute of Technology, Karnataka, Surathkal, Mangalore, India. The results are compared with ANN and Adaptive Neuro-Fuzzy Inference System (ANFIS) models in terms of correlation coefficient, root mean square error and scatter index. Performance of GA-SVMR is found to be reliably superior. b-spline kernel function performs better than other kernel functions for the given set of data.

1. Introduction

Floating breakwaters are well accepted in recent years because of their basic advantages, such as, flexibility, easy mobilization, installation, and retrieval. The system can be fabricated in land, towed to the site, and installed along any desired alignment with ease. In addition, they have several desirable characteristics, such as, comparatively small capital cost, adoption to varying harbour shapes and sizes, short construction time and freedom from silting and scouring. Floating breakwaters could also be utilized to meet location changes, extent of protection required or seasonal demand. They can be used as a temporary protection for offshore activities in hostile environment during construction, drilling works, salvage operation, etc. Hence, it is necessary to study a detailed investigation of proposed floating breakwater.

Several researchers in the past have carried out experimental and numerical investigations on different types of floating breakwaters, such as, Horizontal, sloping, A-type, Y-type, Cage, Pontoon, Tires, Pipes [1–11]. However, there is a lack of a simple mathematical model to predict breakwater performance characteristics, such as the transmission coefficient, which is defined as the ratio of the transmitted wave height past the breakwater to the incident wave height on the breakwater. It is also found that most of the numerical methods have been attempted on simple box-type rectangular floating breakwaters or spar buoy floating breakwaters. These studies are carried out considering a floating breakwater in basic form with some assumptions common in hydrodynamics, which shows less improvement. Till now, there has not been available a simple mathematical model to predict a wave transmission through floating breakwaters by considering all the boundary conditions. Also, for floating pipe breakwaters the energy dissipation process depends on various other factors like pipe interference effect, the spacing between the pipes and number of layers. As the effect of all these factors on transmission and forces in the moorings is not clearly understood, it will be extremely difficult to quantify them mathematically. Still it is a complex problem.

Computational intelligence techniques, such as, Artificial Neural Networks (ANN), Fuzzy logic (FL), Genetic Programming (GP), Support Vector Machines (SVMs) or combinations of these techniques are successfully used to solve complex problems associated with coastal/ocean engineering. Among these techniques, ANN is widely

* Corresponding author.
E-mail addresses: sanras5@gmail.com (S.G. Patil), smandal@nio.org (S. Mandal), arkalvittal@gmail.com (A.V. Hegde).

0965-9978/$ - see front matter © 2011 Elsevier Ltd. All rights reserved.
doi:10.1016/j.advengsoft.2011.09.026

used in coastal/ocean engineering to predict ocean wave parameters like wave height, wave period, impact wave force [12–15]. The most significant features of neural networks are the extreme flexibility due to learning ability and the capability of non-linear function approximations. This has made ANN very popular in recent years, and further this technique has provided promising results in prediction of tidal levels [16], damages to coastal structures [17], depth of eroded caves in a seawall [18], seabed liquefaction [19], storm surges [20], etc. According to Shahidi and Mahjoobi [21] ANNs are not as, transparent as, semi-empirical regression based models. In addition, neural network approach needs to find network parameters, such as, number of hidden layers and neurons by trial and error, which is time consuming. To overcome the problems inherent in ANN training procedures Jeng et al. [19] adopted the concept of genetic algorithm based training of ANN models, which provided accurate results for determining maximum liquefaction depth in a real world application. It is also noticed that apart from improving the performance of ANN, computational effort and time needed for training and testing the model is significantly reduced compared to traditional methods [17].

When the performance of ANN alone is poor in mapping input–output relation, many researchers developed hybrid models by combining ANN with fuzzy system, ANN with numerical wave modeling [22–24], adaptive neuro-fuzzy inference system by Sylaios et al. [23] for wind wave modeling, model trees by Shahidi and Mahjoobi [21] for prediction of significant wave height, etc., for example. ANN is a low level computational structure that performs well when dealing with raw data. The pure feed-forward back propagation learning process could easily be trapped into the local minima.

Recently fuzzy inference systems have become popular in solving complex engineering problems and are widely used in coastal/ocean engineering. However, fuzzy systems lack the ability to learn and cannot adjust themselves. Inspired by the idea of basing the fuzzy logic inference procedure on a feed forward network structure, Jang [25] proposed a fuzzy neural network model – the Adaptive Neuro-Fuzzy Inference System (ANFIS), which is a five-layer feed-forward neural network, which includes fuzzification layer, rule layer, normalization layer, defuzzification layer and a single summation neuron. It is a hybrid neuro-fuzzy technique that brings learning capabilities of neural networks to fuzzy inference system. An ANFIS uses a hybrid learning algorithm that combines the least-squares method and gradient descent principle [25,26]. This hybrid model attracted many researchers to solve complex problems associated with coastal/ocean engineering [22,27–29]. Ozger and Sen [30] have adopted dynamic fuzzy approach to identify the effect of wind speed on wave characteristics variations in ocean wave generating system. Bakhtyar et al. [31] have concluded that the ANFIS model is more flexible than the FIS model, with more options for incorporating the fuzzy nature of the real world system. Sylaios et al. [23] have used Takagi–Sugeno [32] rule based fuzzy inference system for forecasting wave parameters based on the wind speed, direction and the lagged wave characteristics. They used subtractive clustering method to identify the initial and final antecedent fuzzy membership functions. Yagci et al. [33] have used fuzzy logic method in breakwater damage ratio estimation. Erdik [34] has applied fuzzy logic approach in design of conventional rubble mound structures. Apart from above computational intelligence techniques, many authors have used various new approaches to solve complex coastal engineering problems like genetic programming by Gaur and Deo [35] for real time wave forecasting, Guven et al. [36] for prediction of circular pile scour.

SVMs are the recently developed learning techniques that have gained enormous popularity in the field of classification, pattern recognition and regression. SVM works on structural risk minimization principle that has greater generalization ability and is superior to the empirical risk minimization principle as adopted in conventional neural network models. Han et al. [37] applied SVM for flood forecasting, Radhika and Shashi [38] for prediction of atmospheric temperature, Msiza et al. [39] used ANN and SVR for water demand prediction, Rajasekaran et al. [40] developed a Support Vector Machine Regression (SVMR) model for forecasting storm surges. They compared these results with numerical methods and ANN, which indicated that storm surges and surge deviations are efficiently predicted using SVMR. According to Mahjoobi and Mosabbeb [41], SVM creates a more reliable model with better generalization error, in comparison to ANN, they also reveal that SVMs do not over-fit, while ANNs may face such problem and need to deal with it.

Soft computing tools are used for other applications as discussed above. However, it is observed that there are hardly any applications of SVMs on wave transmission of floating breakwater. This fact leads us to use SVM models in this work. In the present paper, the performance of GA-SVMR models for predicting wave transmission coefficient of HIMMFPB is investigated. GAs are used to optimize the SVMR and kernel parameters. Results of GA-SVMR models are compared with that of ANN and ANFIS models.

The paper is organized as follows: Section 1 starts with literature associated with floating breakwaters and applications of soft computing techniques in coastal engineering. Section 2 details wave transmission of floating breakwater and experimental HIMMFPB. Fundamentals of SVMR, GAs for parameter selection and proposed GA-SVMR are detailed in Section 3. Results and discussion are described in Section 4. Conclusions is presented in Section 5.

2. Wave transmission of floating breakwater

The design of floating breakwater is based on the principle that the wave energy is concentrated at the surface in deep water and the same energy is concentrated at below the surface in shallow water, which is to be dissipated. Therefore different types of floating breakwaters like Box, Pontoon, Mat, Tethered float and Pipe are becoming popular. The basic concept by which floating breakwater reduces wave energy include reflection, dissipation, interference and conversion of the energy into non-oscillatory motion. The prime factor in the construction of floating breakwater is to make the width of the breakwater in the direction of wave propagation greater than one-half the wavelength and preferably as wide as incident wavelength. Otherwise, the breakwater rides over the top of the wave without attenuating it. Pontoon and Box types of floating breakwaters belong to the category in which the wave attenuation is achieved by reflecting the wave energy. Mat and Tethered belong to the other category, in which wave energy dissipation is mainly due to drag from the resultant float in motion. Pipe breakwaters mainly dissipate the wave energy, and also partly reflect and transmit the waves. For effective reflection, the breakwater should remain relatively motionless and penetrate to a depth sufficient to prohibit appreciable wave energy from passing underneath.

2.1. Experimental HIMMFPB model setup and data used

The development of floating breakwaters by various investigations has been influenced by certain important features; large masses, large moment of inertia, and the combinations of two. Most of the literature indicates that the parameter "relative width" influences greatly the wave attenuation characteristics of the breakwater. The details of the HIMMFPB are shown in Fig. 1 [42–45]. The breakwater comprises of the rigid Poly Vinyl Chloride (PVC) pipes. These pipes are placed parallel to each other with certain spacing

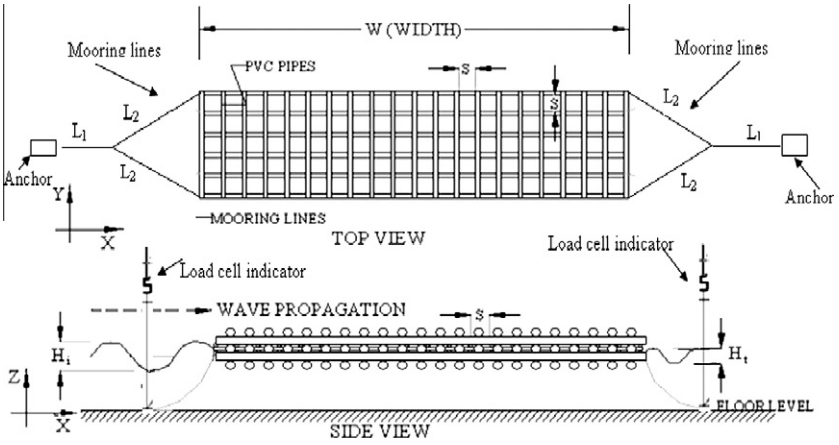

Fig. 1. HIMMFPB model setup.

Table 1
Range of wave-specific and structure-specific parameters used in HIMMFPB.

Wave-specific parameters	Experimental range
Incident wave height, H_i (mm)	30, 60, 90, 120, 150, 180
Wave period, T (s)	1.2, 1.4, 1.6, 1.8, 2.0, 2.2
Depth of water, d (mm)	400, 450, 500
Structure-specific parameters	*Experimental range*
Diameter of pipes, D (mm)	32
Ratio of spacing to diameter of pipes, S/D	2, 3, 4 and 5
Relative breakwater width, W/L	0.4–2.65
Number of layers, n	5

between them in each layer and the adjacent layers are oriented at right angles to each other, so as to form an interlacing. Longitudinal pipes are placed along the direction of propagation of waves and transverse pipes are placed and tied perpendicular to longitudinal pipes. The length of the longitudinal pipes defines the width of the breakwater. It is felt that with proper number of layers, spacing of pipes and relative breakwater width, it is possible to achieve a considerable and effective attenuation of waves. Fig. 1 shows a pictorial representation of the HIMMFPB model in plan and section.

The wave-specific parameters and structure-specific parameters considered in the experiments are shown in Table 1. The experimental study carried out by Kamat [45] shows hydrodynamic characteristics of horizontally interlaced three and five layer floating breakwater systems, in which wave transmission is less for five layer systems. These experimental data are divided into two sets, one for training and other for testing the GA-SVMR models (Table 2). The input parameters that influence the wave transmission (K_t) of floating breakwater, such as, spacing of pipes relative to pipe diameter (S/D), breakwater width relative to wave length (W/L), incident wave relative to water depth (H_i/d), incident wave relative to wave length (H_i/L) are used to train GA-SVMR models as shown in Table 2.

Experimental data on W/L, H_i/d, S/D, H_i/L and K_t are shown in Fig. 2. From this experimental data, first 2131 data points are used to train GA-SVMR models and the remaining 813 data points are used for testing the models.

3. Hybrid Genetic Algorithm Tuned Support Vector Machine Regression (GA-SVMR)

3.1. Fundamentals of Support Vector Machine Regression (SVMR)

Vapnik [46] proposed the Support Vector Machines (SVMs), which is based on statistical learning theory. The basic idea of support vector machines is to map the original data x into a feature space with high dimensionality through a non-linear mapping function and construct an optimal hyper-plane in new space. Hence, given a set of data $S = \{(x_i, d_i)\}_{i=1}^{N}$, where x_i is the input data set, d_i is the desired result, and N corresponds to the size of the data set. Then, according to Smola and Scholkopf [47], the SVM regression function is expressed as

$$y = f(x) = w_i\phi_i(x) + b \tag{1}$$

where $\phi_i(x)$ is the non-linear function in feature of input x, and both w_i and b are coefficients, which are estimated by minimizing the regularized risk function as expressed below:

$$\text{Minimize} : R(C) = \frac{1}{2}\|w\|^2 + C\frac{1}{N}\sum_{i=1}^{N} L_\varepsilon(d_i, y_i) \tag{2}$$

where

$$L_\varepsilon(d_i, y_i) = \begin{cases} |d_i - y_i| - \varepsilon, & |d_i - y_i| \geqslant \varepsilon, \\ 0, & \text{others}, \end{cases} \tag{3}$$

The first term in Eq. (2) is called regularized term, measures the flatness of the function. The second term is the empirical error measured by the ε – insensitive loss function, which is defined as Eq. (3). C and ε are user determined parameters, d_i is the actual value at period i, y_i is the forecasted value at period i, and C is a weighing parameter considered to specify the trade-off between the empirical risk and model flatness. Eq. (3) defines a range where the loss will be zero if the forecasted value is within the ε – tube (Eq. (3) and Fig. 3). However, if the value is out of the ε – tube then the loss is the absolute

Table 2
Data used for training and testing the GA-SVMR models with input parameters.

Model	Input parameters	Number of data points for training	Number of data points for testing
GA-SVMR (linear) GA-SVMR (polynomial) GA-SVMR (rbf) GA-SVMR (erbf) GA-SVMR (spline) GA-SVMR (b-spline)	(S/D), (W/L), (H_i/d), (H_i/L)	2131	813

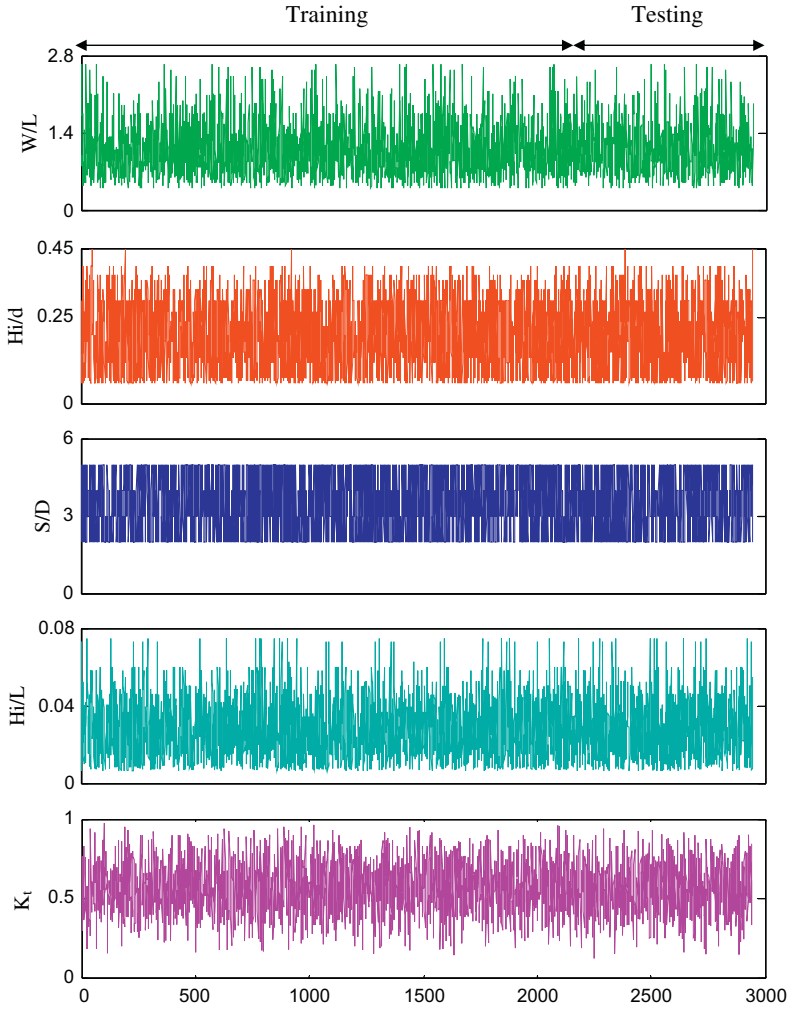

Fig. 2. Experimental data on W/L, H_i/d, S/D, H_i/L and K_t.

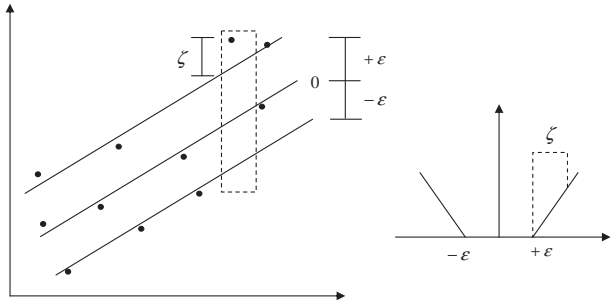

Fig. 3. The loss margin setting corresponds to one dimensional linear SV machine.

value, which is the difference between forecasted value and ε. Introducing two positive slack variables ζ_i and ζ_i^* in Eq. (3), it is possible to transform it into a primal objective function given by:

$$\text{Minimize}: R(w,\zeta_i,\zeta_i^*) = \frac{1}{2}\|w\|^2 + C\sum_{i=1}^{N}(\zeta_i+\zeta_i^*) \tag{4}$$

subject to the constraints;

$d_i - w_i\phi(x_i) - b \leqslant \varepsilon + \zeta_i,$

$w_i\phi(x_i) + b - d_i \leqslant \varepsilon + \zeta_i^*,$

where $\zeta_i, \zeta_i^* \geqslant 0, i = 1,2,\ldots,N.$

ζ_i and ζ_i^* represents the distance from the actual values to the corresponding boundary values of ε-tube.

The key idea is to construct the Lagrange function from the primal objective function and corresponding constraints by introducing the dual set of variables,

$$\begin{aligned} L(w_i,\zeta_i,\zeta_i^*,\alpha_i,\alpha_i^*,\beta_i,\beta_i^*) = {} & \frac{1}{2}\|w\|^2 + C\sum_{i=1}^{N}(\zeta_i+\zeta_i^*) \\ & - \sum_{i=1}^{N}\alpha_i[w_i\phi(x_i)+b-d_i+\varepsilon+\zeta_i] \\ & - \sum_{i=1}^{N}\alpha_i^*[d_i - w_i\phi(x_i) - b + \varepsilon + \zeta_i^*] \\ & - \sum_{i=1}^{N}(\beta_i\zeta_i + \beta_i^*\zeta_i^*) \end{aligned} \tag{5}$$

Eq. (5) is minimized with respect to primal variables w_i, b, ζ, ζ^*, and maximized with respect to non-negative Lagrangian multipliers $\alpha_i, \alpha_i^*, \beta_i$ and β_i^*.

Finally, Karush–Kuhn–Tucker conditions are applied to the regression, and Eq. (5) thus yields the dual Lagrangian,

$$J(\alpha_i, \alpha_i^*) = \sum_{i=1}^{N} d_i(\alpha_i - \alpha_i^*) - \varepsilon \sum_{i=1}^{N} (\alpha_i + \alpha_i^*) - \frac{1}{2} \sum_{i=1}^{N} \sum_{j=1}^{N} (\alpha_i - \alpha_i^*)\left(\alpha_j - \alpha_j^*\right) K(x, x_i) \quad (6)$$

subject to the constraints;

$$\sum_{i=1}^{N} (\alpha_i - \alpha_i^*) = 0, \quad 0 \leqslant \alpha_i \alpha_i^* \leqslant C, \quad i = 1, 2, \ldots, N.$$

In Eq. (6), α_i and α_i^* are called Lagrangian multipliers that satisfy equalities, $\alpha_i \times \alpha_i^* = 0$. After calculating α_i and α_i^*, an optimal desired weights vector of the regression hyper-plane is represented as

$$w^* = \sum_{i=1}^{N} (\alpha_i - \alpha_i^*) K(x_i, x_j) \quad (7)$$

Therefore, the regression function is expressed as,

$$f(x, \alpha, \alpha^*) = \sum_{i=1}^{N} (\alpha_i - \alpha_i^*) K(x_i, x_j) + b \quad (8)$$

Here, $K(x_i,x_j)$ is called the kernel function. The value of the kernel equals the inner product of two vectors x_i and x_j in the feature space $\varphi(x_i)$ and $\varphi(x_j)$, i.e., $K(x_i,x_j) = \varphi(x_i) \times \varphi(x_j)$. The role of the kernel function simplifies the learning process by changing the representation of the data in the input space to a linear representation in a higher-dimensional space called a feature space. A suitable choice of kernel allows the data to become separable in the feature space despite being non-separable in the original input space. This allows us to obtain non-linear algorithm from algorithms previously restricted in handling linearly separable data sets. The function that satisfies Mercer's condition by Vapnik [48] can be used as the kernel function.

In the present paper, we have experimented with the six kernels as shown in Table 3. The linear kernel function is used for linear SVM model, whereas the polynomial, radial basis function (rbf), exponential radial basis function (erbf), spline and b-spline kernels are used for non-linear SVM models. According to Karatzoglou and Meyer [49], Gaussian radial basis function kernel is the general purpose kernel used when there is no prior knowledge about the data. The linear kernel is useful, when dealing with large sparse data vectors, as usually the case in text categorization. The polynomial kernel is popular in image processing, whereas, the spline kernels typically perform well in regression. Selection of two kernel parameters (d,γ) and support vector machine parameters (C,ε) of a SVM model is significant in accuracy of the forecasting, where, the parameter d represents the degree of polynomial and b-spline kernel functions, whereas, γ is the width of rbf and erbf kernel functions. The generalization performance of GA-SVMR depends on a good setting of C, ε and kernel parameters d and γ. Parameter C determines the trade-off between the model complexity (flatness) and the degree to which deviations larger than ε tube [50,51]. If C is too large (infinity), then the objective is to minimize the empirical risk only, without regard to the model complexity [52]. In the present study, quadratic loss function is used. The main idea of using this loss function is to ignore the errors, which are situated within the certain distance of the true value. Parameter ε controls the width of the ε – insensitive zone, which is used to fit the training data. The number of support vectors (*nsv*) used to construct regression function depends on ε, the big ε, the fewer support vectors are selected and results in data compression [53].To optimize these parameters for better generalization of SVM model, SVM model is hybridized with GAs. Section 3.2 details the genetic algorithm in parameter selection, whereas Section 3.3 details interface of genetic algorithm with support vector machine regression to obtain the best GA-SVMR model.

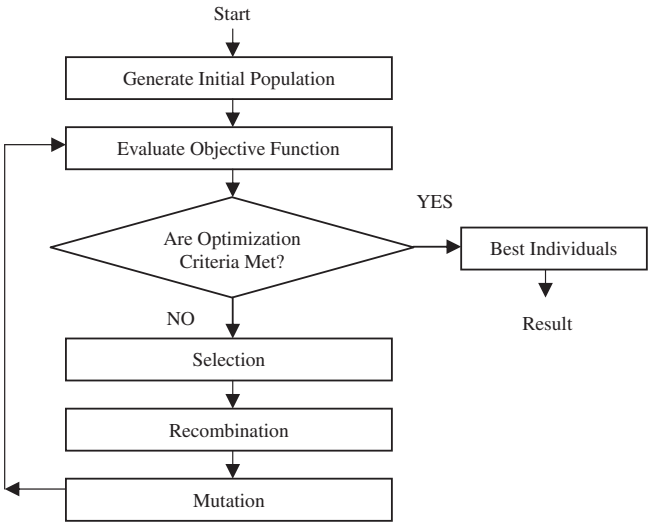

Fig. 4. GAs procedure.

3.2. Genetic algorithm for selecting parameters in the SVMR model

Genetic algorithms are search methods based on principles of natural selection and genetics [54]. The algorithm is based on the principle of the survival of the fittest, which tries to retain genetic information from generation to generation. In this paper, GAs is used to search for better combination of C, ε and kernel parameters (d and γ) to maximize the generalization performance of SVMR model. The procedure of genetic algorithms in parameter selection is shown in Fig. 4, whereas Fig. 5 shows the proposed GA-SVMR model. The codes are written in MATLAB 7 Release 14. The steps involved in GA for selecting SVMs and kernel parameters are as follows:

Table 3
Kernel Functions.

Kernels	Functions	User defined kernel parameter
Linear	$K(x_i, x_j) = a_1 x_i x_j + a_2$	For simplicity set $a_1 = 1$, $a_2 = 0$
Polynomial	$K(x_i, x_j) = ((x_i, x_j) + 1)^d$	d
rbf	$K(x_i, x_j) = \exp\left(-\frac{\|x_i - x_j\|^2}{2\gamma^2}\right)$	γ
erbf	$K(x_i, x_j) = \exp\left(-\frac{\|x_i - x_j\|}{2\gamma^2}\right)$	γ
Spline	$K(x_i, x_j) = 1 + (x_i, x_j) + \frac{1}{2}(x_i, x_j)\min(x_i, x_j) - \frac{1}{6}\min(x_i, x_j)^3$	–
b-Spline	$K(x_i, x_j) = B_{2d+1}(x_i - x_j)$	d

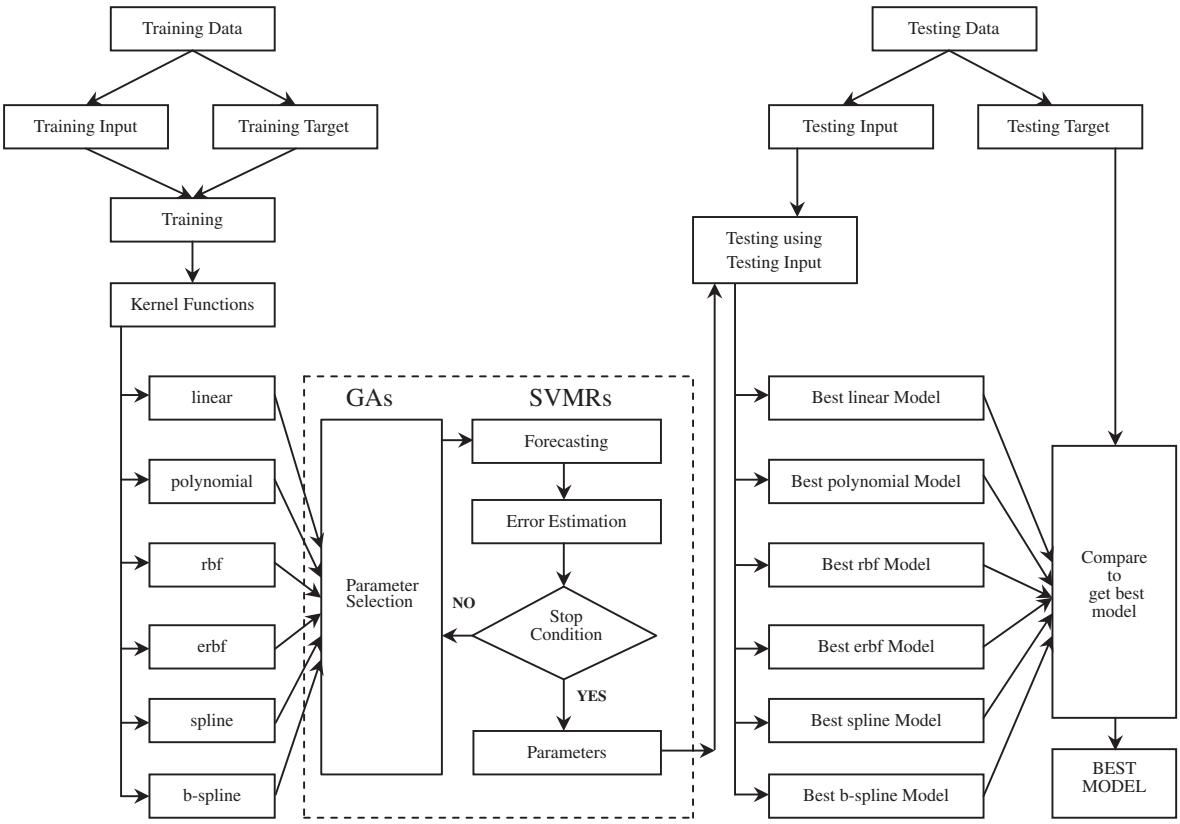

Fig. 5. Flow chart of GA-SVMR.

Step 1. (Initialization): In the present paper initial population of chromosomes is generated randomly. Population size is set to 50. The chromosomes are real coded string, consist of SVMs parameters C, ε and kernel parameters (d and γ).

Step 2. (Evaluating fitness): In this step fitness of each chromosome is evaluated. In the present paper, a negative normalized mean square error is used as the fitness function, which is defined as:

$$\text{Fitness Function} = \frac{1}{-\sigma^2 N}\sum_{i=1}^{N}(d_i - y_i)^2 \tag{9}$$

where

$$\sigma^2 = \frac{1}{N}\sum_{i=1}^{N}(d_i - \overline{d_i})^2$$

N is the total number of data in the test set, $\overline{d_i}$ is the mean of the actual value, d_i is the actual value, and y_i is the predicted value.

Step 3. (New population): In this step new population is created by repeating following steps until the new population is complete.

(i) [Selection]: In the present study, two parent chromosomes from a population are selected according to fitness function (Eq. (9)). The roulette wheel selection principle [54] is used to select chromosomes for reproduction.

(ii) [Crossover]: Here with crossover probability crossover of the parents is done to form new offspring's (children). In cross over, chromosomes are paired randomly. The intermediate crossover principle is used and offspring's are produced according to the following rule.

$$\text{Offspring} = \text{parent1} \pm \alpha(\text{parent2} - \text{parent1}) \tag{10}$$

Table 4
Optimal parameters for GA-SVMR models with different kernels.

Kernel	*nsv*	*C*	ε	γ	*d*
Linear	2131	100	0.001	–	–
Polynomial	2131	96	0.001	–	6
rbf	2131	150	0.001	0.3	–
erbf	2131	6	0.001	1	–
Spline	2131	40,000	0.05	–	–
b-Spline	2131	15	0.05	–	2

where α is the scaling factor chosen uniformly at random over an interval $[-d, 1 + d]$. In the present study d is chosen as 0.25.

(iii) [Mutation]: After cross over operation is performed the string is subjected to mutation operation, this is to prevent falling all solutions of the population into local optimum of solved problem. The variable in the string to be mutated is selected randomly, where incremental operator is used. The rate of crossover and mutation is determined by probabilities. In the present paper, the probabilities of crossover and mutation are set to 0.8 and 0.05 respectively.

(iv) [Accepting]: Accept and place new offspring in the new population.

Step 4. (Replace): Here new generated population is used for a further run of the algorithm.

Step 5. (Stop condition): If the end condition is satisfied, stop, and return the best solution in current population. Otherwise,

Step 6. (Loop): Go to *step 2*.

3.3. The proposed GA-SVMR model

In the present study, MATLAB support vector machine toolbox [50] is interfaced with genetic algorithm to optimize the SVMs

Table 5
GA-SVMR models with statistical measures.

Model	CC train	CC test	Train data		Test data	
			RMSE	*SI*	*RMSE*	*SI*
GA-SVMR (linear)	0.8964	0.8924	0.07072	0.12375	0.07245	0.12925
GA-SVMR (polynomial)	0.9568	0.9513	0.04638	0.08116	0.04946	0.08824
HGASVMR (rbf)	0.9563	0.9478	0.04662	0.08157	0.05119	0.09133
HGASVMR (erbf)	0.9640	0.9416	0.04253	0.07443	0.05412	0.09655
HGASVMR (spline)	0.9834	0.9735	0.02896	0.05068	0.03671	0.06549
GA-SVMR (b-spline)	0.9897	0.9741	0.02286	0.03900	0.03629	0.06474

and kernel parameters simultaneously for better generalization of the proposed GA-SVMR model. Six GA-SVMR models were developed by using six kernel functions (Table 3). In order to study, the performance of each kernel in predicting wave transmission of HIMMFPB, GA-SVMR is trained by applying these kernel functions. For training, experimental data set is used (Fig. 2) and is divided into two groups one for training and other for testing (Table 2). Fig. 5 illustrates the proposed GA-SVMR model. In the first stage training input, training target, kernel function, and range of kernel and SVM parameters are fed to the system. GA generates the initial population that would be used to find optimum factors of kernel functions and SVMs. In the second stage, the system performs typical SVM process using assigned value of the factors in the chromosomes, and calculates the performance of each chromosome. The performance of each chromosome is calculated using fitness function for GAs given in Eq. (9).

In the present study, the main goal is to find the best parameters that produce the most accurate prediction. If the calculated fitness value satisfies the terminal condition in GAs, then the optimal parameters are selected, otherwise, the new generation of the population is produced by applying genetic operators, such as, selection, crossover, and mutation. After the production of new generation, the training process with calculation of the fitness value is performed again. From this point, stage two and stage three are iterated again and again until the stopping conditions are satisfied. Once the stopping condition is satisfied, the genetic search

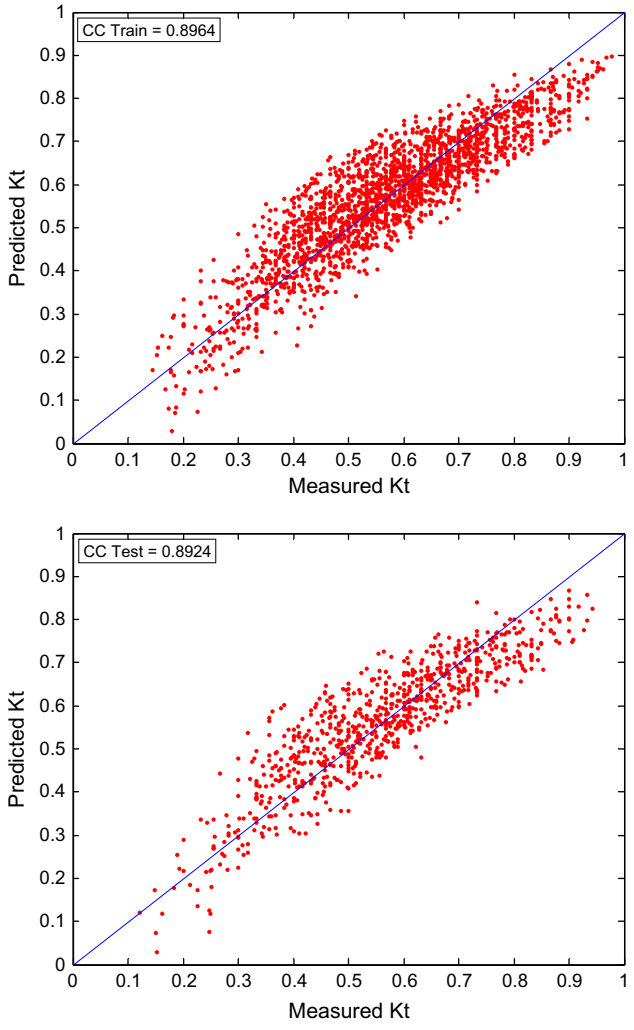

Fig. 6. Comparison of predicted and measured K_t for GA-SVMR (linear) model.

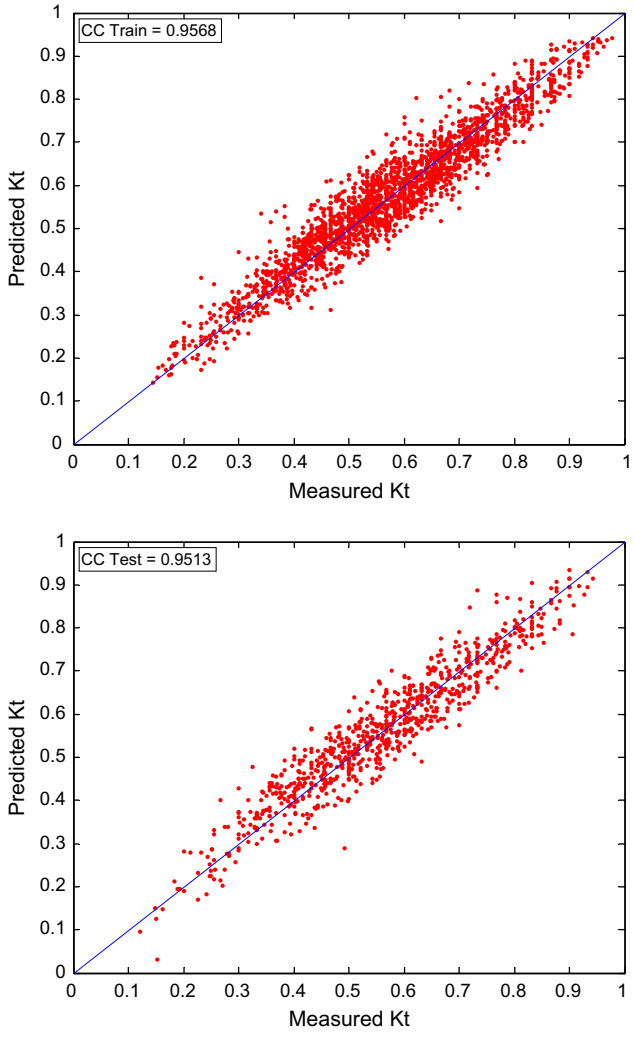

Fig. 7. Comparison of predicted and measured K_t for GA-SVMR (polynomial) model.

finishes and the chromosomes that shows the best performance in the last population is selected as the final result. These optimize SVMs and kernel parameters are shown in Table 4. In the forth and final stage optimized parameters obtained by GA are tested with the test data. The final decision about the optimum models is not based on the training data, but on the testing data, as illustrated in Fig. 5. Once the testing is over, the six models with linear, polynomial, rbf, erbf, spline and b-spline kernels are compared based on statistical measures to get the best model.

4. Results and discussion

To study the effectiveness of the approach, statistical comparison of measured and predicted values of K_t, correlation coefficient (CC) is used, which is defined as

$$CC = \frac{\sum_{i=1}^{N}(K_{tmi} - \overline{K_{tm}})(K_{tpi} - \overline{K_{tp}})}{\sqrt{\sum_{i=1}^{N}(K_{tmi} - \overline{K_{tm}})^2} \times \sqrt{\sum_{i=1}^{N}(K_{tpi} - \overline{K_{tp}})^2}} \quad (11)$$

where K_{tmi} and K_{tpi} represents the measured and predicted wave transmission coefficient, respectively, $\overline{K_{tm}}$ and $\overline{K_{tp}}$ are the mean value of measured and predicted observations, N is the number of observations. Higher the CC value better is the agreement between the measured and predicted values of K_t. Apart from this, other statistical measures computed are root-mean-square error (*RMSE*), and scatter index (*SI*). These are defined as

$$RMSE = \sqrt{\frac{1}{N}\sum_{i-1}^{N}(K_{tmi} - K_{tpi})^2} \quad (12)$$

$$SI = \frac{RMSE}{\overline{K_{tm}}} \quad (13)$$

Statistical measures computed using train and test data for GA-SVMR are shown in Table 5. Train and test data are used to compare the models results. The trained and test results (CCs) of six models are shown in Table 5 and Figs. 6–11.

In comparison to all models, linear kernel function shows poor generalization performance (CC Train = 0.8964 and CC Test = 0.8924) in prediction of K_t for HIMMFPB with *SI*, 0.12375 and 0.12925 for train and test data respectively. Number of support vectors used in GA-SVMR with linear kernel function is 2131, which is 100%. Similarly, GA-SVMR with non-linear kernel functions also used 100% of support vectors, which indicates that every training input is utilized as support vector. This clearly proves that, there is no noise in the training data set, but there is non-linearity and complexity associated in mapping input and output parameters of HIMMFPB. Increasing the C will disturb the solution, but it can be helpful for other kernels like spline kernel, where C is 40,000 as shown in Table 4. In case of b-spline kernel C is 15,

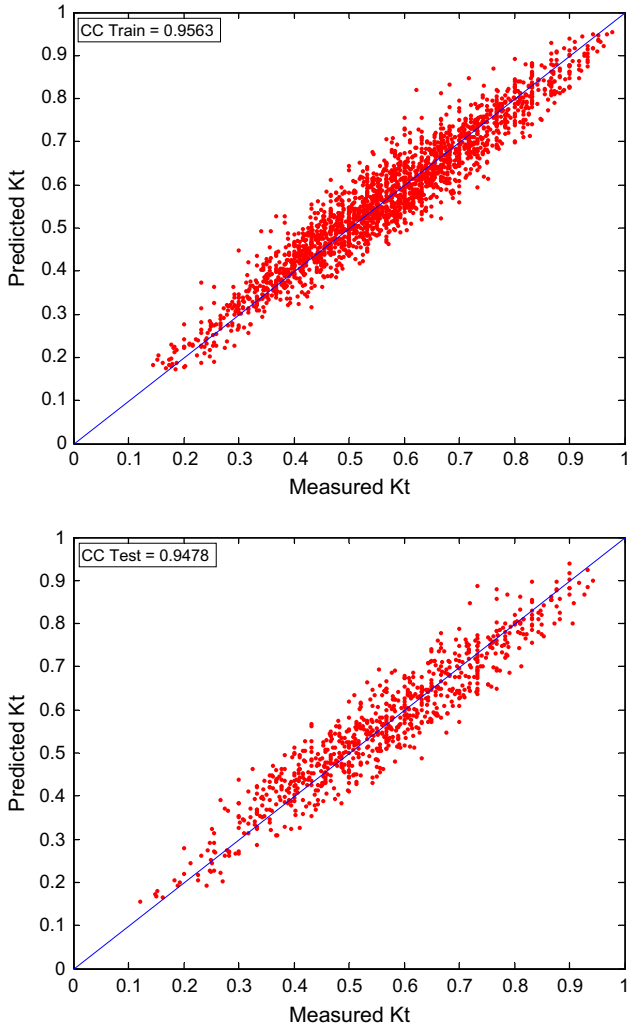

Fig. 8. Comparison of predicted and measured K_t for GA-SVMR (rbf) model.

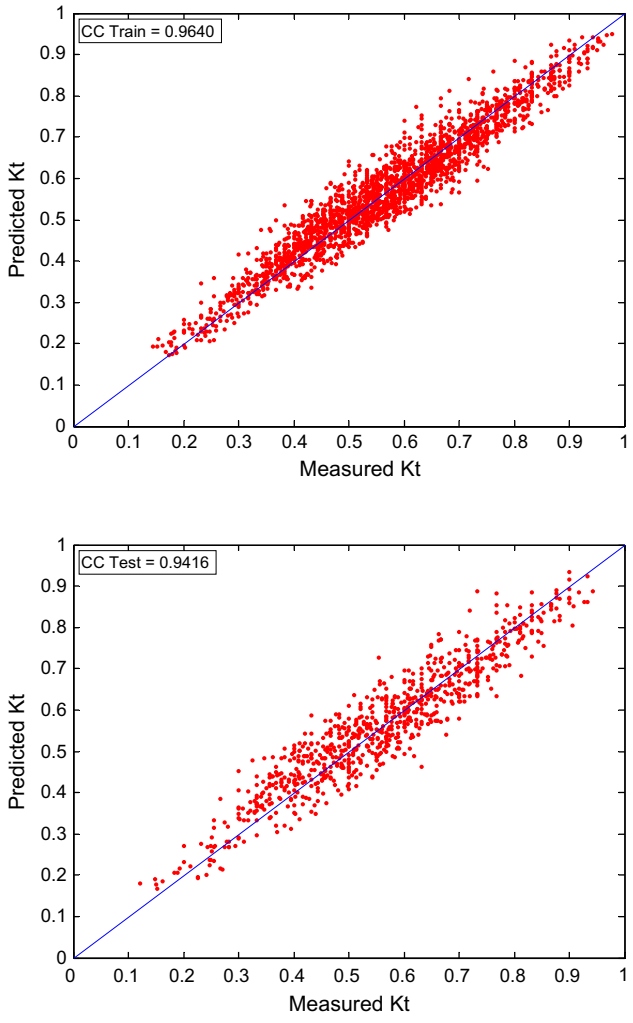

Fig. 9. Comparison of predicted and measured K_t for GA-SVMR (erbf) model.

whereas for erbf it is 6. For polynomial and linear kernel it is 96 and 100 respectively. A b-spline kernel function has better generalization performance with *RMSE* 0.02286 and 0.03629 for train and test data respectively. Whereas, similar trend is shown by spline kernel function with slightly higher *RMSE* 0.02896 and 0.03671 for train and test data respectively.

Correlation coefficient of GA-SVMR(b-spline) model (CC Train = 0.9897 and CC Test = 0.9741) is slightly better than GA-SVMR(spline) model, but considerably better than GA-SVMR(linear) model, whereas the performance of GA-SVMR(polynomial) model is better than GA-SVMR(rbf) and GA-SVMR(erbf) models with *SI* 0.08824 for test data, whereas, for rbf and erbf kernels it is 0.09133 and 0.09655 respectively. In comparison to GA-SVMR model with b-spline and spline kernel functions, *SI* and *RMSE* is very high for GA-SVMR models with linear and erbf kernel function for test data (Table 5). It is noticed that the performance of these models depends on the better selection of SVM and kernel parameters. In case of polynomial kernel, the degree of the function d, when low; the function estimation is very bad, however, for higher d, performance is good. The optimal value of d in case of polynomial kernel function obtained by GAs is 6 and for b-spline kernel function it is 2. The optimal width (γ) obtained by GAs in case of rbf and erbf kernel functions are 0.3 and 1 respectively. Kernel and SVM parameters obtained by GA (Table 4) is tested by using test data sets (Table 2), which show

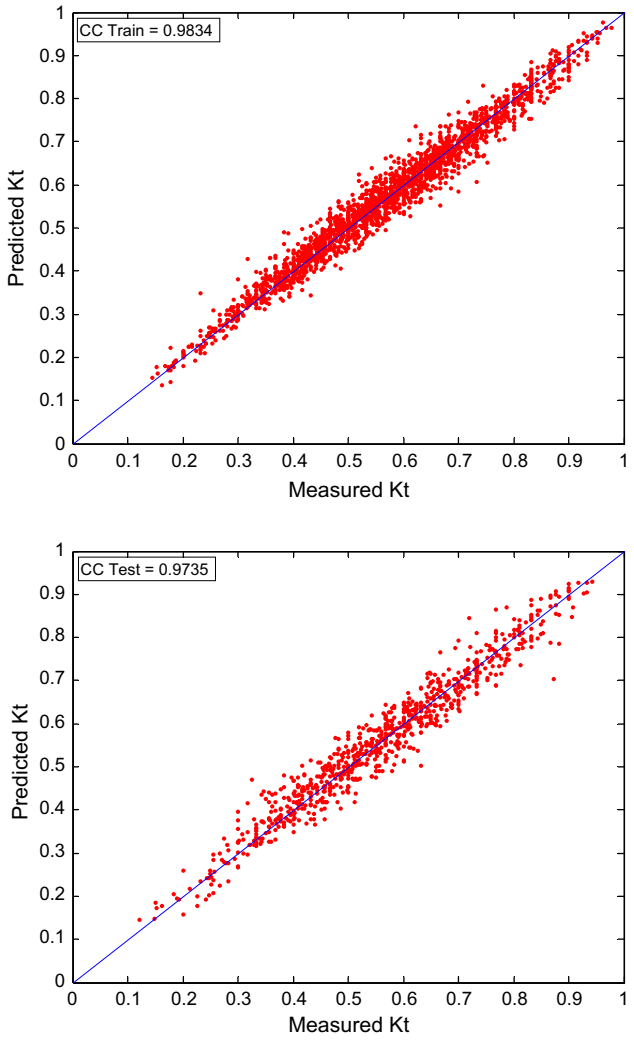

Fig. 10. Comparison of predicted and measured K_t for GA-SVMR (spline) model.

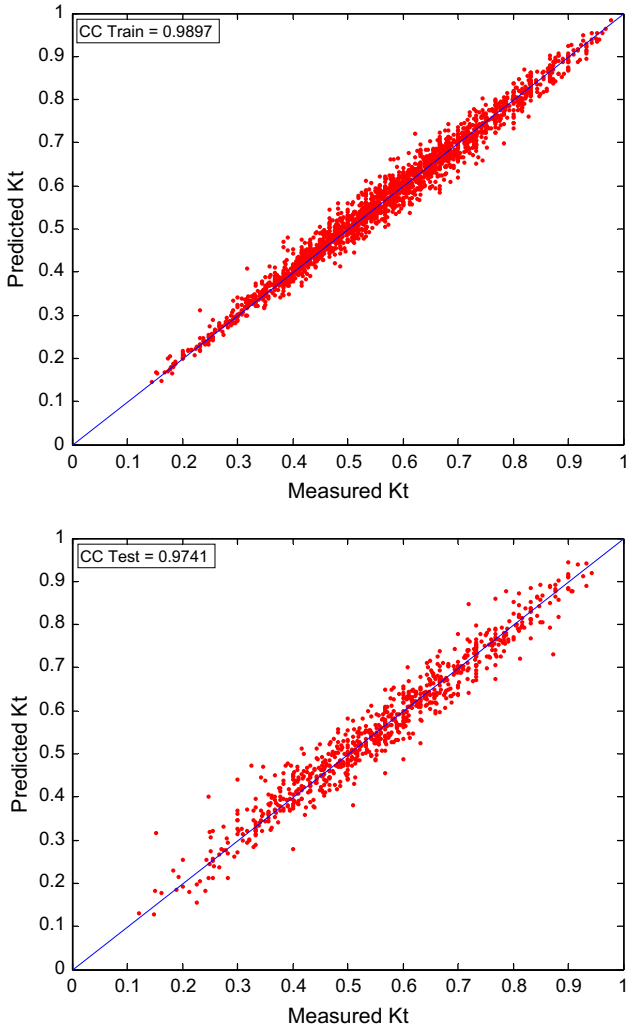

Fig. 11. Comparison of predicted and measured K_t for GA-SVMR (b-spline) model.

Table 6
ANN and ANFIS models with statistical measures.

Model	CC train	CC test	Train data		Test data	
			RMSE	*SI*	*RMSE*	*SI*
ANN [55]	0.9537	0.9488	0.05176	0.09058	0.05395	0.09625
ANFIS [56]	0.9723	0.9635	0.03727	0.06522	0.04307	0.07683

better generalization performance with highest CC Test = 0.9741 for GA-SVMR (b-spline) model.

The same data set has been used for estimating K_t using ANN [55] and ANFIS [56]. CCs, *SI* and *RMSE* of K_t are shown in Table 6. From Table 5 and 6, it is observed that the GA-SVMR (b-spline) model yields higher CCs as compared to that of ANN and ANFIS models, whereas *RMSE* and *SI* values are higher in ANN and ANFIS models as compared to GA-SVMR (b-spline) model. However the GA-SVMR model with linear kernel function has shown poor generalization, whereas, ANFIS model perform better than GA-SVMR models with polynomial, rbf and erbf kernel functions.

In SVM regression, the solution is unique for specific loss function, kernel type, and SVM and kernel parameters. If we run the same program, the results will be exactly the same. The model is much more complex and cannot be used in other implementations, whereas the results will not be same in case of ANN and ANFIS models.

5. Conclusions

An application of hybrid genetic algorithm tuned support vector machine regression for prediction of wave transmission for HIMMFPB is presented in this paper. Our proposed model optimizes SVMs and kernel parameters simultaneously. The performance of GA-SVMR models is compared with ANN and ANFIS models. The results obtained shows that GA-SVMR with b-spline kernel functions performs better than ANN and ANFIS models.

The forecasting performance of GA-SVMR appears to be highly influenced by the choice of its kernel function, and the good setting of kernel and SVM parameters. The b-spline kernel function performed superior than other kernel.

It is also observed that parameter selection in the case of GA-SVMR has a significant effect on the performance of the model.

GA-SVMR can replace the ANN and ANFIS based models for wave transmission prediction of HIMMFPB.

GA-SVMR can be utilized to provide a fast and reliable solution in prediction of the wave transmission for HIMMFPB, thereby making GA-SVMR as an alternate approach to map the wave structure interactions of HIMMFPB.

Acknowledgements

The authors are grateful to the Director, and Head, Department of Applied Mechanics and Hydraulics, NITK, Surathkal, India for support and encouragement provided to them and for permission to publish the paper. Thanks are also due to Ministry of Earth Sciences, GOI for sponsoring the project on HIMMFPB at NITK, Surathkal, India.

References

[1] Bishop TC. Floating tire breakwater design comparison. J Water-way, Port, Coast Ocean Eng, ASCE 1982;108:421–6.
[2] Harms VW. Design criteria for floating tire breakwater. J Waterway, Port, Coast Ocean Eng, ASCE 1979;106:149–70.
[3] Harris AJ, Webber NB. A floating breakwater. In: Proceedings of the 11th Coastal Engineering Conference, London, England; 1968. p. 1049–54.
[4] Homma M, Horikawa K, Mochizuki H. An experimental study of floating breakwaters. In: Proceedings of the 10th Coastal Engineering Conference, Japan; 1964. p. 85–94.
[5] Kennedy RJ, Marsalek J. Flexible porous floating breakwater. In: Proceedings of the 11th Coastal Engineering Conference, London, England; 1968. p. 1095–103.
[6] Leach AP, McDougal GW, Solitt KC. Hinged floating breakwater. J Waterway, Port, Coast Ocean Eng, ASCE 1985;111:895–920.
[7] Mani JS. Design of *Y* – frame floating breakwater. J Waterways, Port, Coast Ocean Eng, ASCE 1991;117:105–18.
[8] McCartney LB. Floating breakwater design. J Waterway, Port, Coast Ocean Eng, ASCE 1985;111:304–18.
[9] Murali K, Mani JS. Performance of cage floating breakwater. J Waterway, Port, Coast Ocean Eng, ASCE 1997;123:172–9.
[10] Sannasiraj SA, Sundar V, Sundaravadivelu R. Mooring forces and motion response of pontoon-type floating breakwaters. Ocean Eng 1998;25:27–48.
[11] Sundar V, Sundaravadivelu R, Purushotham S. Hydrodynamic characteristics of moored floating pipe breakwater in random waves. Proc Inst Mech Eng, J Eng Maritime Environ 2003;217:95–108.
[12] Deo MC, Jha A, Chaphekar AS, Ravikant K. Neural networks for wave forecasting. Ocean Eng 2001;28:889–98.
[13] Deo MC, Jagdale SS. Prediction of breaking waves with neural networks. Ocean Eng 2003;30:1163–78.
[14] Gunaydin K. The estimation of monthly mean significant wave heights by using artificial neural network and regression methods. Ocean Eng 2008;35:1406–15.
[15] Londhe SN, Deo MC. Wave tranquility studies using neural networks. Marine Struct 2003;16:419–36.
[16] Chang HK, Lin LC. Multi-point tidal prediction using artificial neural network with tide-generating forces. Coastal Eng 2006;53:857–64.
[17] Mandal S, Rao S, Manjunatha YR. Stability analysis of rubble mound breakwater using ANN. In: Proceedings of the Indian National Conference on Harbour and Ocean Engineering, INCHOE, NITK, Surathkal, India; 2007. p. 551–60.
[18] Lee TL, Tsai CP, Lin HM, Fang CJ. A combined thermo graphic analysis – neural network methodology for eroded caves in a sea wall. Ocean Eng 2009;36:1251–7.
[19] Jeng DS, Cha D, Blumenstein M. Neural network for the prediction of wave induced liquefaction potential. Ocean Eng 2004;31:2073–86.
[20] Tseng CM, Jan CD, Wang JS, Wang CM. Application of artificial neural networks in typhoon surge forecasting. Ocean Eng 2007;34:1757–68.
[21] Shahidi EA, Mahjoobi J. Comparision between M5' model tree and neural network for prediction of significant wave height in lake superior. Ocean Eng 2009;36:1175–81.
[22] Kazeminezhad MH, Etemad-shahidi A, Mousvi SJ. Application of fuzzy inference system in the prediction of wave parameters. Ocean Eng 2005;32:1709–25.
[23] Sylaios G, Bouchette F, Tsihrintziz VA, Denamiel C. A fuzzy inference system for wind wave modeling. Ocean Eng 2009;36:1358–65.
[24] Malekmohamadi I, Ghiassi R, Yazdanpanah MJ. Wave hindcasting by coupling numerical model and artificial neural networks. Ocean Eng 2008;35:417–25.
[25] Jang JSR. ANFIS: adaptive-networked-based fuzzy inference systems. IEEE Trans Syst, Man, Cybern 1993;23:665–85.
[26] Jang JSR, Sun CT, Mizutani E. Neuro-fuzzy and soft computing. PTR Prentice Hall; 1997.
[27] Bakhtyar R, Yeganeh-Bakhtiary A, Ghaheri A. Application of neuro-fuzzy approach in prediction of run-up in swash zone. Appl Ocean Res 2008;30:17–27.
[28] Bateni SM, Jeng DS. Estimation of pile group scours using adaptive neuro-fuzzy approach. Ocean Eng 2007;34:1344–54.
[29] Chang H-K, Chien W-A. A fuzzy – neural hybrid system of simulating typhoon waves. Coast Eng 2006;53:737–48.
[30] Ozger M, Sen Z. Prediction of wave parameters by fuzzy logic approach. Ocean Eng 2006;34:460–9.
[31] Bakhtyar R, Ghaheri A, Yeganeh-Bakhtiary A, Baldock TE. Longshore sediment transport estimation using a fuzzy inference system. Appl Ocean Res 2008;30:273–86.
[32] Takagi T, Sugeno M. Fuzzy identification of systems and its applications to modeling and control. IEEE Trans Syst, Man, Cybern 1985;15:116–32.
[33] Yagci O, Mercan DE, Cigizoglu HK, Kabdasli MS. Artificial intelligence methods in breakwater damage ratio estimation. Ocean Eng 2005;32:2088–106.
[34] Erdik T. Fuzzy logic approach to conventional rubble mound structure design. Expert Syst Appl 2009;36:4162–70.
[35] Gaur S, Deo MC. Real-time wave forecasting using genetic programming. Ocean Eng 2008;35:1166–72.
[36] Guven A, Azamathulla HMd, Zakaria NA. Linear genetic programming for prediction of circular pile scours. Ocean Eng 2009;36:985–91.
[37] Han D, Chan L, Zhu N. Flood forecasting using support vector machines. J Hydroinformatics 2007;09.4:267–76.
[38] Radhika Y, Shashi M. Atmospheric temperature prediction using support vector machines. Int J Comput Theory Eng 2009;1:55–8.
[39] Msiza IS, Nelwamonda FV, Marwala T. Water demand prediction using artificial neural networks and support vector regression. J Comput 2008;3:1–8.
[40] Rajasekaran S, Gayathri S, Lee TL. Support vector regression methodology for storm surge prediction. Ocean Eng 2008;35:1578–87.
[41] Mahjoobi J, Mosabbeb EA. Prediction of significant wave height using regressive support vector machines. Ocean Eng 2009;36:339–47.
[42] Deepak JC. Laboratory investigations on horizontal interlaced multi-layer moored floating pipe breakwater [M.Tech thesis]. Department of Applied Mechanics and Hydraulics, NITK, Surathkal, Karnataka, India; 2006.
[43] Hegde AV, Kamath K, Magadum AS. Performance characteristics of horizontal interlaced multilayer moored floating pipe breakwater. J Waterway, Port, Coast Ocean Eng, ASCE 2007;133:275–85.
[44] Jagadisha YS. Laboratory investigations on horizontal interlaced multi-layer moored floating pipe breakwater model [M. Tech thesis]. Department of Applied Mechanics and Hydraulics, NITK, Surathkal, Karnataka, India; 2007.
[45] Kamat K. Hydrodynamics performance characteristics of horizontal interlaced multi-layer moored floating pipe breakwater – a physical model study [Ph.D. Thesis]. Department of Applied Mechanics and Hydraulics, NITK, Surathkal, Karnataka, India; 2010.
[46] Vapnik V. Statistical leaning theory. New York: John Wiley and Sons; 1998.
[47] Smola AJ, Scholkopf B. A Tutorial on support vector regression. Neuro COLT Technical Report NC-TR-98-030, Royal Holloway College. University of London, UK; 1998.
[48] Vapnik V. The nature statistic leaning theory. New York: Springer-Verlag; 1995.
[49] Karatzoglou A, Meyer D. Support vectors machines in R. J Stat Softw 2006;15:1.
[50] Gunn SR. Support vector machines for classification and regression. University of Southampton, Technical report, Image speech and intelligent Systems group; 1998.
[51] Smola A. Regression estimation with support vector learning machines. Technische Universitat Munchen; 1996.
[52] Cherkassky V, Ma Y. Practical selection of SVM parameters and noise estimation for SVM regression. Neural Networks 2004;17:113–26.
[53] Kecman V. Learning and soft computing, support vector machines, neural networks, and fuzzy logic models. Cambridge, MA, USA: The MIT Press; 2001.
[54] Holland JH. Adaption in natural and artificial system. Massachusetts: The MIT Press; 1975.
[55] Mandal S, Patil SG, Hegde AV. Wave transmission prediction of multilayer floating breakwater using neural network. In: Proceedings of international conference in ocean engineering. IIT Madras, Chennai, India; 2009. p. 574–85.
[56] Patil SG, Mandal S, Hegde AV, Srinivasan A. Neuro-fuzzy bases approach for wave transmission prediction of horizontally interlaced multilayer moored floating pipe breakwater. Ocean Eng 2011;38:186–96.